Use of delay and sum for sparse reconstruction improvement for structural health monitoring

Nokhbatolfoghahai, Ali; Navazi, Hossein M.; Groves, Roger M.

Important note
To cite this publication, please use the final published version (if applicable).
Please check the document version above.

Use of delay and sum for sparse reconstruction improvement for structural health monitoring

Ali Nokhbatolfoghahai[1], Hossein M Navazi[1] and Roger M Groves[2]

Abstract

To perform active structural health monitoring, guided Lamb waves for damage detection have recently gained extensive attention. Many algorithms are used for damage detection with guided waves and among them, the delay-and-sum method is the most commonly used algorithm because of its robustness and simplicity. However, delay-and-sum images tend to have poor accuracy with a large spot size and a high noise floor, especially in the presence of multiple damages. To overcome these problems, another method that is based on sparse reconstruction can be used. Although the images produced by the sparse reconstruction method are superior to the conventional delay-and-sum method, it has the challenges of the time and cost of computations in comparison with the delay-and-sum method. Also, in some cases in multi-damage detection, the sparse reconstruction method totally fails. In this article, using prior support information of the structure achieved by the delay-and-sum method, a hybrid method based on sparse reconstruction method is proposed to improve the computational performance and robustness of sparse reconstruction method in the case of multi-damage presence. The effectiveness of the proposed method in detecting damages is demonstrated experimentally and numerically on a simple aluminum plate. The technique is also shown to accurately identify and localize multi-site damages as well as single damage with low sampled signals.

Keywords

structural health monitoring, Lamb waves, hybrid method, sparse reconstruction, delay-and-sum

1. Introduction

Structural health monitoring (SHM) has recently received considerable attention as a way for increasing the efficiency of maintenance for end users of structures. SHM can significantly reduce the maintenance cost by replacing the periodic and scheduled maintenance by condition-based maintenance (CBM), which involves continuous real-time monitoring of in-service structures (Balageas et al., 2006). Also, using SHM systems can help manufacturers to save weight, size, and cost of structures by changing the design paradigm to active safety (Giurgiutiu, 2014). SHM system tasks can be classified into five levels, which are (1) damage detection, (2) damage localization, (3) damage assessment, (4) remaining life prediction, and (5) developing smart structures with self-evaluating, self-healing, or control capabilities (Stepinski et al., 2013). It is clear that all of the SHM system tasks that are described here are based on damage interrogation.

There are some ways of performing damage interrogation such as using vibrational and modal properties (Samir et al., 2018; Zhou et al., 2017), monitoring the local or distribution of strain over the structure (Glisic and Inaudi, 2008; Khatir et al., 2019), and using ultrasonic waves. For over a half-century, using ultrasonic waves has become a reliable and accepted method of damage interrogation (Levine, 2014). To perform ultrasonic SHM in plate-like structures, the use of guided waves, for example, Lamb waves, is an attractive method. The Lamb waves are elastic waves that propagate in thin-walled structures and were first described by Lamb (1917). Lamb waves–based SHM systems have some advantages such as (1) the transducers are usually lightweight, cheap, and easily attached to the structures; (2) as the Lamb waves can travel a long

[1]Department of Aerospace Engineering, Sharif University of Technology, Tehran, Iran
[2]Aerospace Non-Destructive Testing Laboratory, Faculty of Aerospace Engineering, Delft University of Technology, Delft, The Netherlands

Corresponding author:
Hossein M Navazi, Department of Aerospace Engineering, Sharif University of Technology, Azadi Ave., PO Box 11155-8639, Tehran 1458889694, Iran.
Email: navazi@sharif.edu

distance with little attenuation, the SHM systems based on them can scan a large area of a structure with a few transducers; (3) they involve high-frequency excitation and ultrasonic waves with small wavelength; therefore, they are sensitive to the small and barely visible internal and external damage (Alleyne and Cawley, 1992); and (4) due to high-frequency excitation, it can be well isolated from low amplitude low-frequency ambient vibration (Mitra and Gopalakrishnan, 2016). However, some drawbacks introduce challenges in the use of Lamb waves in SHM systems such as complexities in analyzing the Lamb waves response, due to their multimodal and dispersion properties (Giurgiutiu, 2005). Early researchers in the field of Lamb waves SHM mainly focused on the damage detection capabilities and behavior of the Lamb waves due to their interaction with damages (Alleyne and Cawley, 1992; Guo and Cawley, 1993; Rose, 2002; Su et al., 2006; Worlton, 1956). After that, some of the damage localization methods were developed including tomography methods (Wright et al., 1997; Zhao et al., 2011), use of phased arrays (Giurgiutiu and Bao, 2004; Giurgiutiu et al., 2011; Purekar et al., 2004), and sparse arrays (Clarke et al., 2010; Michaels and Michaels, 2004; Wang et al., 2004). Among the above-listed methods, the use of sparse arrays of transducers is a commonly proposed configuration because of its low cost and ease of implementation (Clarke et al., 2010; Levine, 2014). The delay-and-sum (DAS) method is one of the methods that is based on the sparse array configuration (Michaels, 2008) that was introduced by Wang et al. (2004). In his work, for the first time, he utilized baseline signals for a sparse array and adapted a well-known radar technique (DAS beamforming) in the context of guided waves and SHM for damage detection and localization. In addition to the DAS method, other localization algorithms have been developed such as the correlation-based approach (Quaegebeur and Masson, 2012), adaptive algorithms such as minimum-variance imaging (Hall and Michaels, 2010), and statistical approaches such as the use of maximum likelihood estimation (Flynn et al., 2011).

Despite all these methods, the DAS method is the most commonly used algorithm because of its robustness and conceptual simplicity. However, the DAS performance tends to be poor with a large spot size and a high noise floor particularly in the presence of multiple damages (Levine and Michaels, 2013). To overcome these problems, a new imaging algorithm was developed, based on the assumption of damage sparsity of a structure and sparse reconstruction (SR) (Golato et al., 2016; Levine and Michaels, 2013, 2014; Sen et al., 2019; Wang et al., 2018). In this method, the structure is divided into some pixels, where most of them are damage free, and just a sparse set of them are assumed to contain damages. Differential signals are decomposed into a sparse linear combination of pre-computed

signals that shows the echoes from all possible damage locations. Using these pre-computed signals, a dictionary matrix is generated, and the SR techniques are applied to achieve this decomposition (Levine and Michaels, 2013). Although the images produced by the SR method are superior to the conventional DAS method (Levine, 2014), it has the challenge of the time and the cost of computations with respect to the DAS method, especially in applications with real-time processing. In the SR method, the generation of the dictionary matrix requires time, disk space, and a large size of dictionary matrix increases execution time and memory usage, while reducing the size of the dictionary leads to a decrease in the accuracy and resolution of images. Also, in images reconstructed through the SR method, the spot size is typically one or two pixels; however, detection can completely fail in the presence of multiple damages (Levine, 2014).

In SR techniques, the conventional approach assumes that the probability of being zero or nonzero is the same for all elements of the unknown vector. However, in many applications, additional prior information is available. This prior information can provide statistical backgrounds to assign the probability of being nonzero to each element of unknown vectors. Some previous works in the field of compressed sensing have introduced the approach to the use of prior support information to optimize the SR algorithm in the application of data recovering and face recognition (Fan et al., 2015; Friedlander et al., 2012; Khajehnejad et al., 2009; Needell et al., 2017).

In this article, using prior information obtained from the robust and quick DAS method, a hybrid method is developed based on SR and DAS methods. Using this hybrid method, the accuracy and resolution of damage detection are improved compared to the individual techniques, especially in the presence of multiple damages. Besides, the computational cost and memory usage are significantly decreased by reducing the time sampling frequency of signals even less than Nyquist rate.

2. Theoretical background

In this section, the theory of the Lamb wave propagation is presented, and then a summary of the mathematical theory of SR methods as well as the hybrid method is presented.

2.1. Lamb waves

In 1917, a British mathematician Horace Lamb introduced elastic waves in plates which are formed due to the interaction of two types of bulk waves (longitudinal and transverse waves) with the boundaries of the plate (Lamb, 1917). A propagating Lamb wave has two classes, symmetric and antisymmetric modes that are

denoted as S_n and A_n, respectively. In this work, to prevent unnecessary complexity in signal processing, a low enough excitation frequency is chosen so that only the S_0 and A_0 modes can exist and higher order modes are eliminated. Also, for excitation of purely single-mode Lamb waves, a pair of piezoelectric patch transducers (PZT) transducers is used in both sides of the plate (Su et al., 2006). For each Lamb wave mode, there is a dispersion curve which shows the phase and group velocity of the modes as a function of the multiplication of excitation frequency and the plate's thickness. For a specific propagating Lamb wave mode, the far-field shape of a cylindrically propagating wave after traveling a distance d can be described as (Levine, 2014)

$$y(t) = \left(\frac{d}{d_{ref}}\right)^{-\frac{1}{2}} F^{-1}\left\{ (F\{x(t)\})exp\left(\frac{-fd2\pi i}{C_p(f)}\right) \right\} \quad (1)$$

where $C_p(f)$ is the phase velocity as a function of frequency f for the given thickness of the plate, $x(t)$ is the excitation time function, and d_{ref} is the reference distance. Also $F\{\}$ denotes the discrete Fourier transform and $i = \sqrt{-1}$. To represent the shape of a propagating wave at point r that is excited by the time function $x(t)$ at the point s regarding equation (1), propagating operator P is defined as

$$y_{s,r}(t) = P_{s\rightarrow r}\{x(t)\} \quad (2)$$

Using these relationships, a wave that is excited at point s interacts with damage at point q and is then received by a sensor at point s and could be described as

$$y_{s,q,r}(t) = \left(\frac{||r-q||_2}{d_{ref}}\right)^{-\frac{1}{2}}\left(\frac{||q-s||_2}{d_{ref}}\right)^{-\frac{1}{2}} F^{-1}\left\{ \left[H(f,\theta_{s,q},\theta_{q,r}) \cdot (F\{x(t)\}(f))exp\left(\frac{-i2\pi f||q-s||_2}{C_p(f)}\right) \right]exp\left(\frac{-i2\pi f||r-q||_2}{C_p(f)}\right) \right\} \quad (3)$$

where $\theta_{a,b} = \angle(b-a)$ and $||\,||_2$ denotes the l_2-norm of a vector. Also, $H(f,\theta_{s,q},\theta_{q,r})$ describes the interaction of the Lamb wave with damage; however, in this work, since there is no prior information about the type of damage, this set is equal to 1.

2.2. SR method

SR refers to optimization techniques for solving the linear underdetermined inverse problem $\mathbf{y} = \mathbf{Ax}$ to calculate $\mathbf{x}$, where the unknown vector $\mathbf{x}$ is assumed to be sparse. Also, $\mathbf{y}$ is the known vector and $\mathbf{A}$ is the dictionary matrix. The imaging method based on SR in SHM is a dictionary-based method and mainly uses the sparsity assumption of structural damages. In this method, subtracted signals are used to evaluate the presence of damage, and for each pair of actuator a and receiver r, the subtracted signal achieved is

$$y_{a,r}(t) = y_{a,r}^{measurment}(t) - y_{a,r}^{baseline}(t) \quad (4)$$

Assuming the linear structure, the subtracted signal is formed from the superposition of different signals due to scatters that can exist at all p pixels of the structure. Therefore, the subtracted signal can be decomposed as

$$y_{a,r}(t) = \sum_{i=1}^{p} x_i a_{a,i,r} \quad (5)$$

where x_i is the unknown coefficient that shows the possibility of damage presence in the pixel i. Also, the $a_{a,i,r}$ is the analytically computed signal that indicates the shape of scattering wave due to the interaction of Lamb wave propagated from point a with a scatterer located at point i and then received by a sensor placed at point r and is calculated as

$$a_{a,i,r}(t) = h(t;\theta_{a,i},\theta_{i,r}) * P_{i\rightarrow r}\{P_{a\rightarrow i}[x(t)]\} \quad (6)$$

where $*$ denotes the convolution operator. This decomposition can be done for all pairs of actuator–sensors. Therefore, for a distributed array of N transducers, the analytically computed signals in equation (6) are repeated for all $N(N-1)$ pairs of sensors that form the linear equation $\mathbf{y} = \mathbf{Ax}$ as

$$\underbrace{\begin{bmatrix} y_{1,2}(t) \\ y_{1,3}(t) \\ \vdots \\ y_{a,r}(t) \\ \vdots \\ y_{N,N-1}(t) \end{bmatrix}_{N(N-1)}}_{y} = \underbrace{\begin{bmatrix} a_{1,1,2} & a_{1,2,2} & \cdots & a_{1,i,2} & \cdots & a_{1,p,2} \\ a_{1,1,3} & a_{1,2,3} & \cdots & & & a_{1,p,3} \\ \vdots & \vdots & \ddots & & \ddots & \vdots \\ a_{a,1,r} & a_{a,2,r} & \cdots & & \cdots & a_{a,p,r} \\ \vdots & \vdots & \ddots & & \ddots & \vdots \\ a_{N,1,N-1} & a_{N,2,N-1} & \cdots & a_{N,i,N-1} & \cdots & a_{N,p,N-1} \end{bmatrix}_{[N(N-1)]p}}_{A} \underbrace{\begin{bmatrix} x_1 \\ x_2 \\ \vdots \\ x_i \\ \vdots \\ x_p \end{bmatrix}_{p}}_{X} \quad (7)$$

where **A** is the dictionary matrix, **y** is the subtracted signals, and the unknown vector **x** shows the location of damages that is assumed to be sparse. In this study, to compensate for the effect of phase shifting, the detected envelope of the subtracted signal and pre-computed signals is used as

$$y'_{a,r}(t) = abs(Hilbert(y_{a,r}(t)))$$
$$d'_{a,i,r}(t) = abs(Hilbert(a_{a,i,r}(t)))$$
(8)

In this work, to solve the linear inverse problem, the basis pursuit denoising (BPDN) method is used as was used by Levine (2014) and Levine and Michaels (2013), which is an l_1-optimization method. This method minimizes the l_1-norm of the vector **x** to solve the optimization problem as

$$\mathbf{x} = \text{argmin} \, ||\mathbf{x}||_1 \, \text{subject to} \, ||\mathbf{y} - A\mathbf{x}||_2 < \sigma \quad (9)$$

where σ is the user-specified parameter that acts as a trade-off parameter between sparsity and reconstruction accuracy.

2.3. Hybrid DAS-SR method

The l_1-minimization problem, which is shown in equation (9), typically does not incorporate any prior information about the unknown vector **x**; however, in SHM applications, it is possible to provide a rough estimation of the status of the structure by performing some cheap and quick evaluations. The DAS method is one of the methods that could provide a rough, robust, and quick estimation of the status of the structure. Also, in the DAS method, the configuration of transducers and hardware, the procedure of measurement signals, and some preprocessing levels are the same as the SR method.

In the case of multi-defects, as stated by Levine (2014), the quality of DAS images may decrease with a large spot, but the detection by the SR method in some cases may totally fail. Also, another comparison performed by Levine (2014) shows that the DAS method is significantly quicker and cheaper than the SR method. The rough comparisons of these two methods can show in some conditions (such as multi-damage existence) the robustness of the DAS method is higher than for SR method; however, its accuracy is lower than for SR. Therefore, these two methods can complement each other, and this gives rise to the idea of using the DAS method to leverage the SR method.

To develop a hybrid DAS-SR method, we need to define support $\tilde{T} \subset \{1, \ldots, p\}$ as a prior support estimate, define weights for each pixel in the structure, and then solve weighted l_1 minimization

$$\mathbf{x} = \text{argmin} \, ||\mathbf{x}||_{1,\vec{w}} \quad \text{subject to} \, ||\mathbf{y} - A\mathbf{x}||_2 < \sigma \quad (10)$$

where $||\mathbf{x}||_{1,\vec{w}}$ is the weighted l_1-norm and is calculated as

$$||\mathbf{x}||_{1,\vec{w}} = \sum_{i=1}^{n} w_i |x_i| \quad \text{and} \quad w_i = \begin{cases} w \in [0,1] & i \in \tilde{T} \\ 1 & i \in \tilde{T}^c \end{cases}$$
(11)

where $\vec{w} = [w_1, w_2, \ldots, w_n]$ is the vector of weights related to unknown vector **x**, which shows pixels of the structure. The logic behind this formula is that choosing a weight w_i less than 1 will encourage x_i being nonzero in the minimizing of equation (10).

To define the support $\tilde{T}$ and weights w_i for each pixel, we should assign a number E_i, which is related to the probability of damage presence. To do this, here we use the results achieved by DAS for each pixel as follows

$$E_i = \frac{1}{N(N-1)} \sum_{a=1}^{N-1} \sum_{r=i+1}^{N} y'_{a,r}(t_{a,i,r}) \quad (12)$$

where $t_{a,i,r}$ is the time of flight for wave propagating from actuator a to the pixel i and then received by sensor r. After finding E_i, we calculate $P_i = E_i/Max(E)$ and set the threshold C_0 to define the support set $\tilde{T} = \{T_1, \ldots, T_i\}$ as

$$\tilde{T}_i \in \{1, \ldots, p\} \quad \text{for } i = 1, \ldots, p \quad \text{where } |P_i| > C_0$$
(13)

As for each index, there is a different level of confidence; we apply different weights corresponding to each index that they are in the support. In this work, to define weights, a relationship is proposed as follows

$$w_i = \frac{1 + \exp(1)}{1 + \exp(1 + 10P_i)} \quad (14)$$

Equation (14) which relates E_i to the weight w_i is an empirical relationship which is roughly estimated by considering various cases with several conditions and some mathematical theories presented by Flinth (2016) and Needell et al. (2017). In equation (14), lower weights are assigned to the pixels with a higher probability of being nonzero. In this work, for DAS calculations, we use the formulations presented by Michaels (2008).

3. Application of the DAS-SR method

In this section, two applications of the proposed hybrid method are studied: the first one is the application of this method for increasing the computational performance using low-frequency sampled signals and the second one is the application of the hybrid method in multi-damage detection.

3.1. Increasing the computational performance

As stated above, the main application of SHM systems is the real-time monitoring of the status of structures.
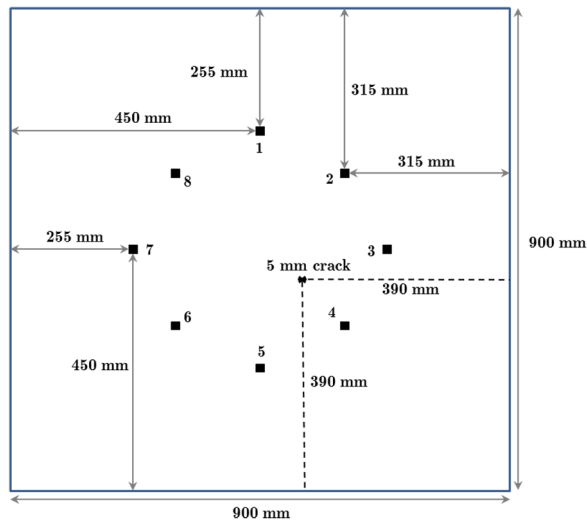
Figure 1. Configuration of the plate with PZT transducers and a crack.

Table 1. Selection of mesh size.

Total number of nodes	Minimum and maximum of NPW	Average NPW	Normalized RMS
165×10^3	$NPW \geqslant 5$ $NPW \leqslant 50$	8	0.375
683×10^3	$NPW \geqslant 8$ $NPW \leqslant 85$	16	0.770
914×10^3	$NPW \geqslant 10$ $NPW \leqslant 110$	19	0.938
1119×10^3	$NPW \geqslant 14$ $NPW \leqslant 110$	21	1
1343×10^3	$NPW \geqslant 16$ $NPW \leqslant 110$	23	0.992
1570×10^3	$NPW \geqslant 17$ $NPW \leqslant 130$	25	0.998

NPW: node per wavelength; RMS: root mean square.

To perform real-time processing, computational performance is an important issue because it could significantly affect the cost of hardware and the operational capability of the SHM systems. In this way, one of the main drawbacks of the SR method is the time and cost of computations in comparison with the DAS method. In the SR method, the size of the dictionary matrix plays an essential role in the computational performance of the method, as a larger dictionary matrix increases excitation time and memory usage, while reducing the size of dictionary leads to a decrease in accuracy of results. In this work, the capability of the hybrid DAS-SR method is evaluated for working with a reduced size dictionary matrix, by reducing the time sampling rate of the measured and pre-computed signals, while the accuracy does not decrease.

3.1.1. Case studies. To verify the application of the hybrid method in reducing the computational cost, numerical simulations, as well as experimental measurements, were performed on a flat 90 cm by 90 cm aluminum plate with 3 mm thickness. Also, to interrogate the structure, a sparse array of eight PZT transducers was used, and simulated damage was placed on the structure. The studied configuration is shown in Figure 1.

In the numerical simulation, the test case shown in Figure 1 was modeled and solved in a commercial finite-element (FE) software (Ansys Workbench 18.2) using the Explicit Dynamic Solver. To generate the mesh, the solid element and mapped face approach as well as multi-zone approach were used. Also, to select a proper mesh size and determine the average number of node per wavelength (NPW), a mesh convergence study was performed on the root mean square (RMS) of signal measured by PZT 1 due to excitation by PZT 5. Table 1 shows the steps of mesh convergence study.

The maximum NPW that is shown in Table 1 is related to the area near the crack, and the minimum NPW is related to the area near the boundaries of the plate. Also, the normalized RMS is the RMS value of each signal that is normalized with respect to the maximum value of RMS among the iterations. After performing mesh study for a plate with a single crack, we used almost 1.2M elements and 1.6M nodes with the average 25 NPW.

In addition, for the simulation of S_0 propagating mode, we have used three elements within the thickness of the structure. Also, 5 mm horizontal cut damage throughout the plate thickness was simulated as a detection target. To generate Lamb waves, square PZT transducers are modeled as a homogeneous material, with a length/width of 10 mm and an infinitesimally thin bonding layer with perfect bonding. The finite element model (FEM) of the plate with the embedded PZTs and the crack is shown in Figure 2.

In addition, experimental testing is performed on an aluminum plate with the same configuration, as shown in Figure 1. In the experimental setup, to simulate the damage, a glued-in steel rod with 6 mm diameter was used in the same position as the analytical model. Also, the transducers were square PZT type PIC255 with the width of 10 mm and thickness of 0.5 mm, and the transducers were bonded on the aluminum plate using superglue. Signal generation was carried out by waveform generator Agilent 33500B, and a wideband voltage amplifier Agilent 33502A was used to amplify the excitation signal. Also, the data acquisition was performed using PicoScope 6402 and standard cables with Bayonet Neill–Concelman (BNC) connectors. The experimental setup is shown in Figure 3.

In both the experimental test and the finite element analysis, for pure S_0 Lamb wave mode generation, a pair of PZT transducers was used in the same location on both sides of the plate, to excite the plate with a

Figure 2. The finite element model of the plate with embedded PZTs and the simulation crack.

(a)   (b)
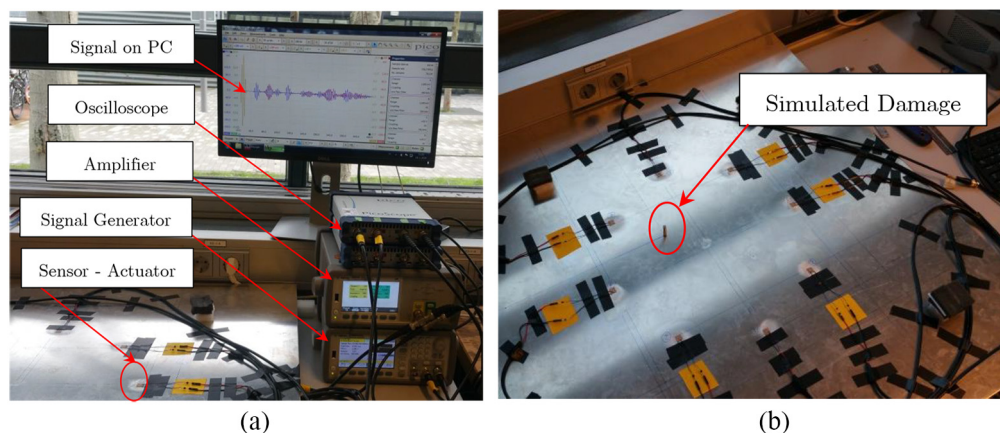
Figure 3. Experimental setup: (a) general setup for data gathering and (b) the plate with simulated damage.

signal with the same shape and phase. Also, to maximize the signal-to-noise ratio (SNR) of the measured signals, a 150 kHz four-cycle Hann-windowed tone burst is used as an excitation signal. Also, to validate the FEM simulations, a comparison between experimental measured and numerical simulated signals for the same actuator and sensor (actuator 6 and sensor 2) is shown in Figure 4.

The excitation signal shown in Figure 4 is normalized to its maximum value and the received signals are normalized with respect to maximum peak of direct waves. The sampling frequency of the experimental signal is much more than FEM simulated signal and this causes some difference in peak values. The difference between RMS of these two signals is about 1% and the difference between the time of flights of direct waves is less than 0.5%.

3.1.2. Results. In this section, the images constructed with different time sampling frequencies through DAS, SR, and hybrid methods are compared. In Figures 5 to 9, the results obtained from the experimental tests are shown.

As it can be seen from Figures 5 to 9, the DAS and SR methods do not work with the signals that are

sampled less than two times of Nyquist rate; however, the hybrid method works successfully with signals that are sampled even less than Nyquist rate. Also, in Figures 10 to 14, the results obtained from the FEM numerical simulation are shown.

The results obtained from the numerical simulations show the similar behavior with those of the experimental tests and both of them prove the capability of the hybrid method to produce accurate results with a smaller size of dictionary matrix than that of the SR method. In addition, the processing times used by SR-DAS method for signals with different sampling frequencies are shown in Table 2. For this computation, a desktop PC with a 64 GB RAM and a processor of CPU E5-1620 v2 3.7 GHz is used and the duration of signals is about 240 μs.

Table 2 only shows the elapsed time in the preprocessing and processing steps and does not include the elapsed time for data transfer to and from memory.

3.2. Multi-damage detection

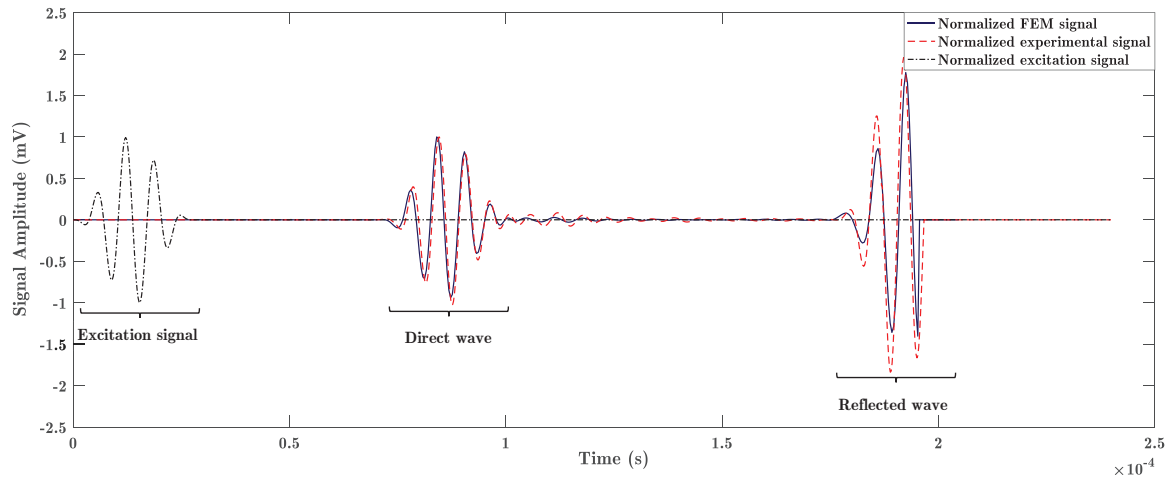One of the weaknesses of both the DAS and SR methods is in the detection of multiple damages,

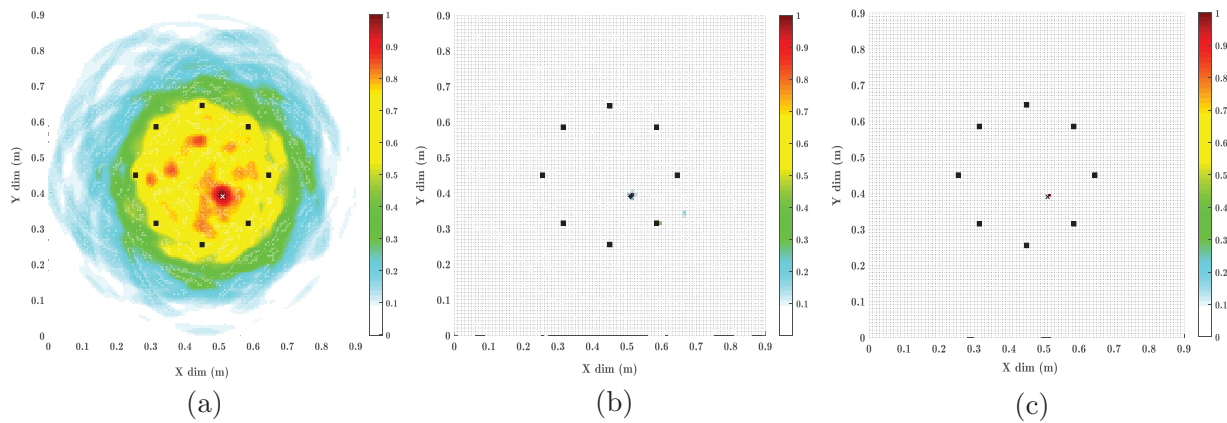**Figure 4.** Comparison between experimental measured and FEM simulated normalized signals for actuator 6 and sensor 2.

Figure 5. Images reconstructed through (a) DAS method, (b) SR method, and (c) hybrid method with the experimental signals sampled at 2.4 MHz (8× Nyquist rate).
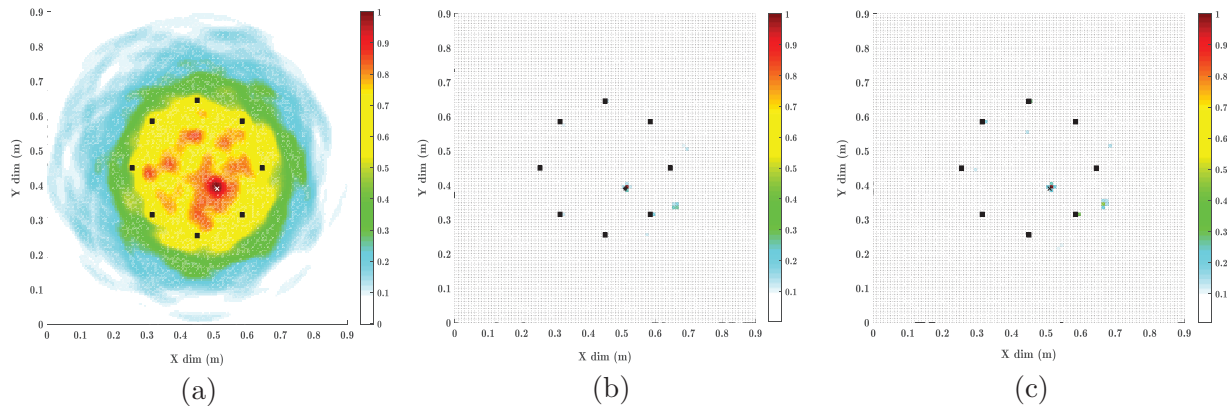

Figure 6. Images reconstructed through (a) DAS method, (b) SR method, and (c) hybrid method with the experimental signals sampled at 1.2 MHz (4× Nyquist rate).

simultaneously. In the DAS method, however, while the general area of the presence of damages can be identified, the detection of the exact location of damages tends to be poor due to the interference of hot

spots. However, in the SR method, the spot size usually is one or two pixels, but in some cases, the detection can totally fail. Therefore, it seems that by combining these two methods in the application of multi-damage
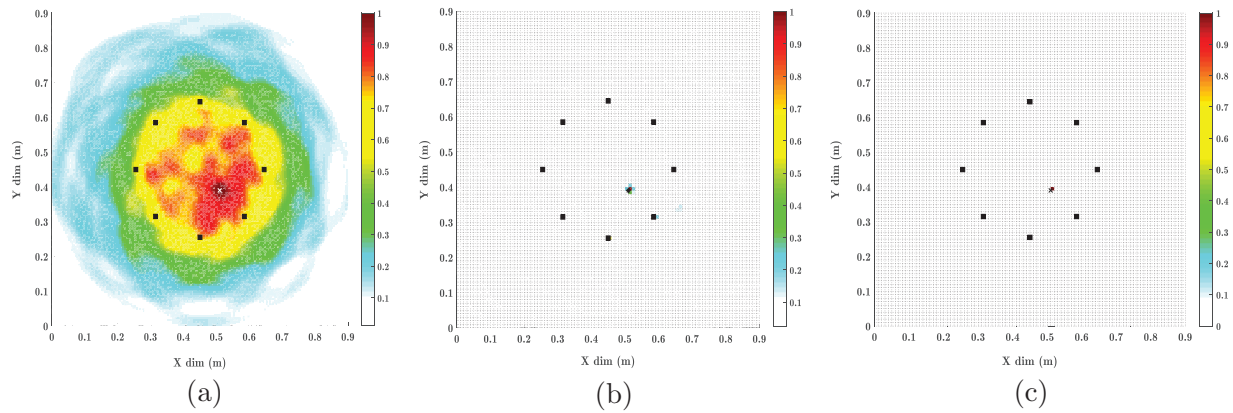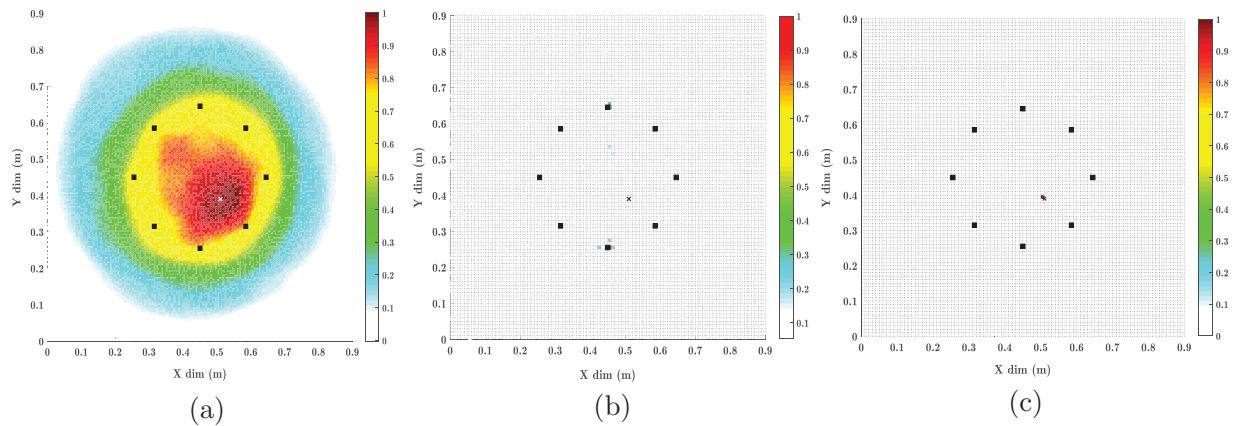
Figure 7. Images reconstructed through (a) DAS method, (b) SR method, and (c) hybrid method with the experimental signals sampled at 600 kHz (2× Nyquist rate).

Figure 8. Images reconstructed through (a) DAS method, (b) SR method, and (c) hybrid method with the experimental signals sampled at 300 kHz (1× Nyquist rate).
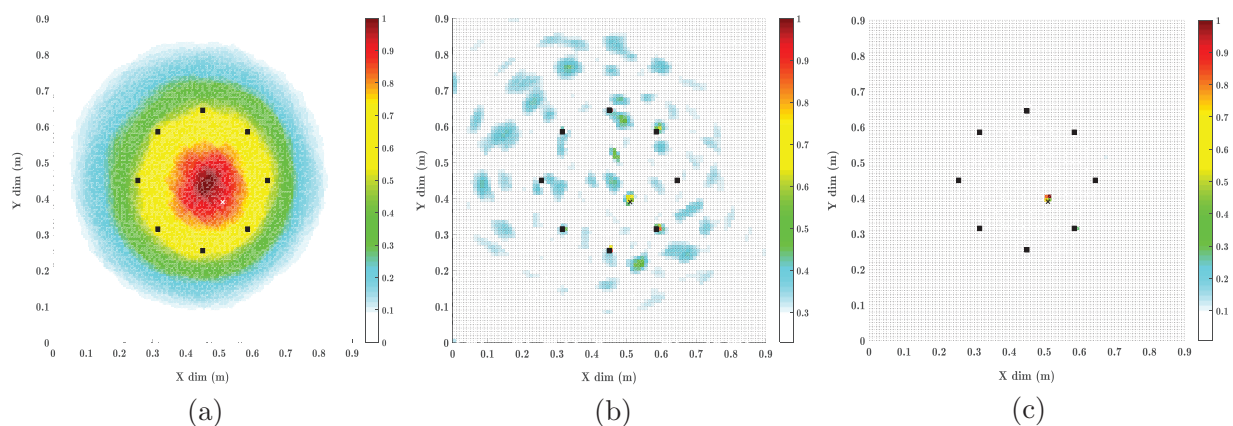

Figure 9. Images reconstructed through (a) DAS method, (b) SR method, and (c) hybrid method with the experimental signals sampled at 150 kHz (1/2× Nyquist rate).

location detection, we can gain from both the robustness of DAS and the accuracy of the SR method.

3.2.1. Case study. In this work, for evaluation of the hybrid method in multi-damage detection, numerical simulation for two damages as well as the experimental test for two and three damages has been performed. For the numerical simulations and experimental tests, a FEM and experimental setup just like those described in section "Case studies" are prepared, with the only
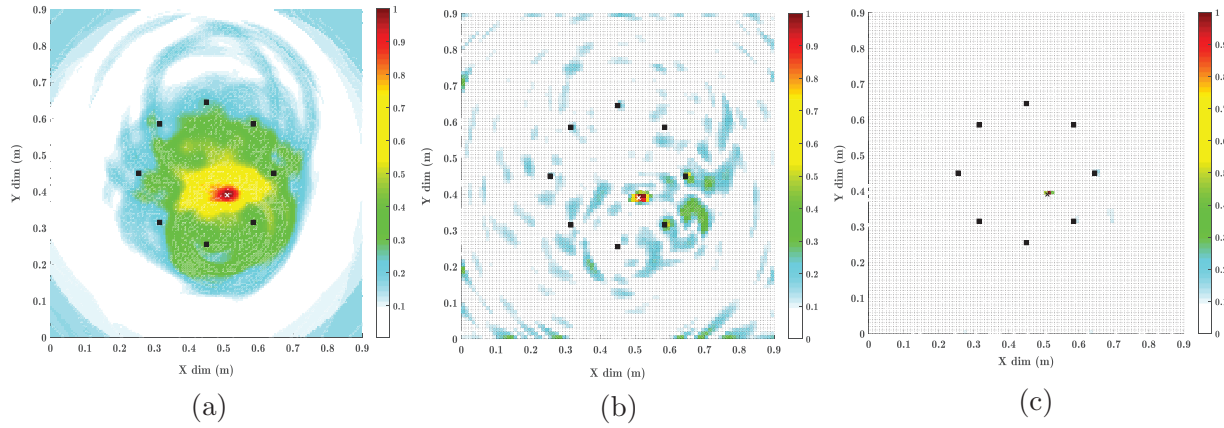
Figure 10. Images reconstructed through (a) DAS method, (b) SR method, and (c) hybrid method with the FEM simulation signals sampled at 2.4 MHz (8× Nyquist rate).
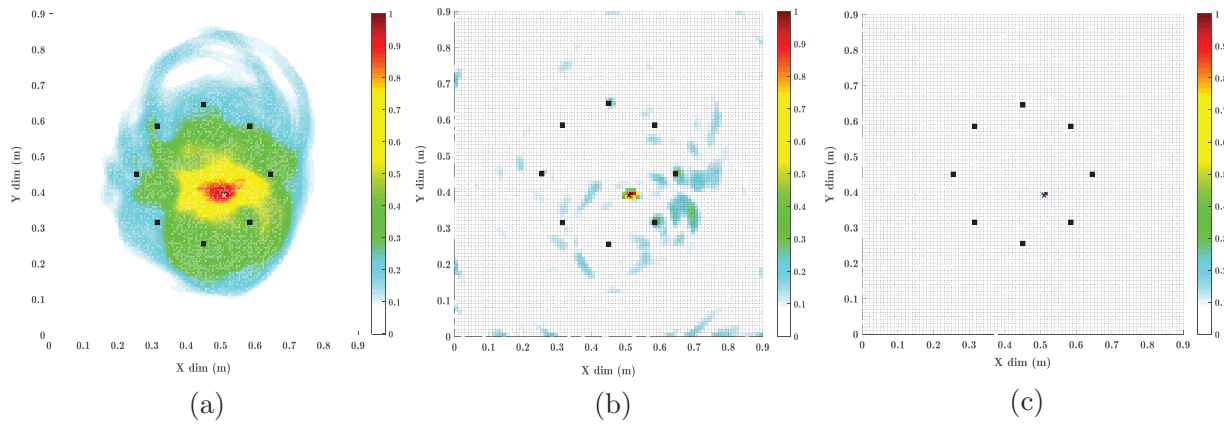

Figure 11. Images reconstructed through (a) DAS method, (b) SR method, and (c) hybrid method with the FEM simulation signals sampled at 1.2 MHz (4× Nyquist rate).
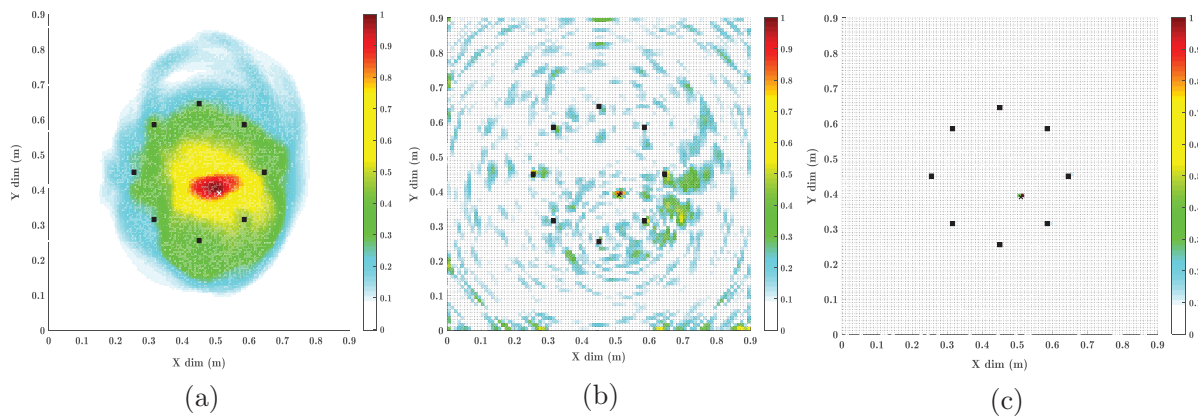

Figure 12. Images reconstructed through (a) DAS method, (b) SR method, and (c) hybrid method with the FEM simulation signals sampled at 600 kHz (2× Nyquist rate).

difference being in the number of damages. The configurations of test cases with two and three damages are shown in Figure 15.

As stated above, for experimental validation, the signal measurements are performed for test setups

with two and three simulated damages, as shown in Figure 16.

3.2.2. Results. In this section, the results achieved by DAS, SR, and hybrid methods are compared for a
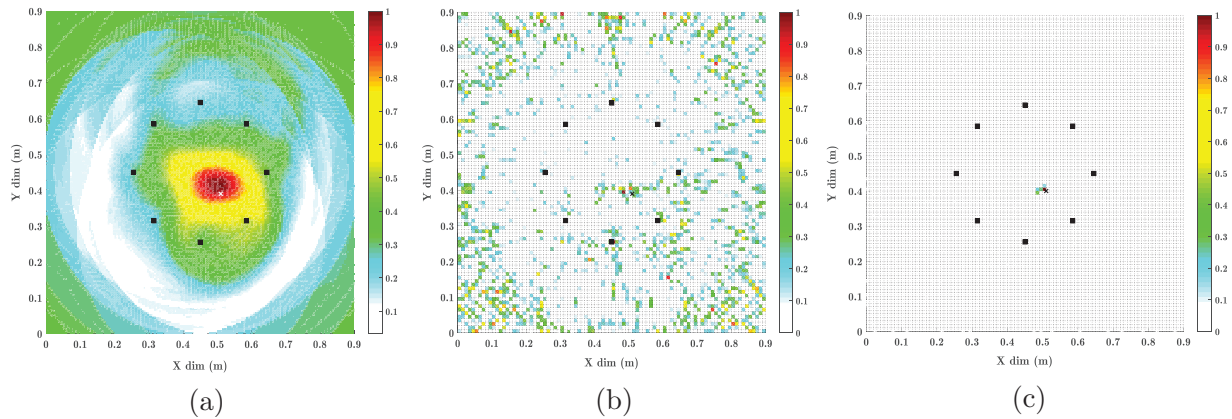
Figure 13. Images reconstructed through (a) DAS method, (b) SR method, and (c) hybrid method with the FEM simulation signals sampled at 300 kHz ($1\times$ Nyquist rate).
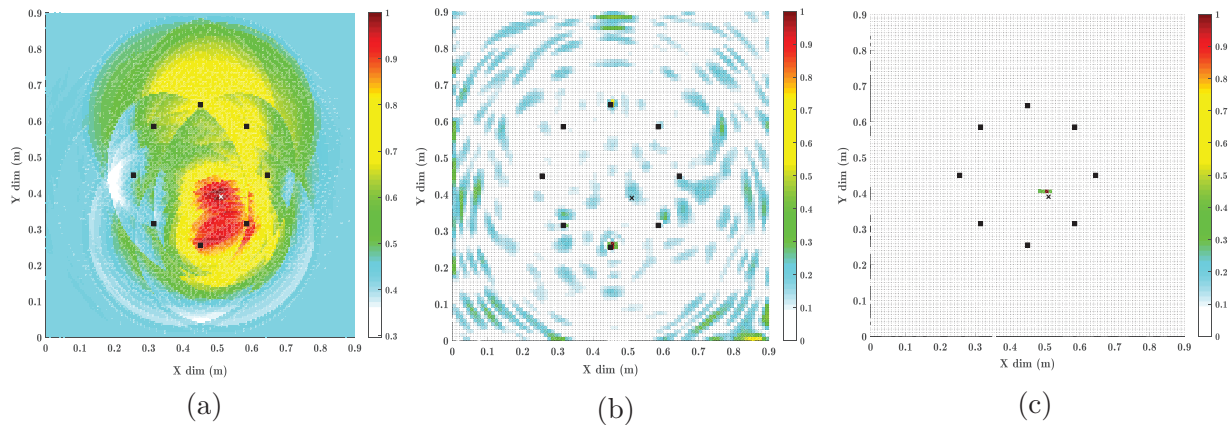

Figure 14. Images reconstructed through (a) DAS method, (b) SR method, and (c) hybrid method with the FEM simulation signals sampled at 150 kHz ($1/2\times$ Nyquist rate).

Table 2. Time elapsed for signals with different sampling ratios using SR-DAS.

Sampling frequency	Processing time for the DAS method (s)	Processing time for the SR method (s)	Processing time for the hybrid SR-DAS method (s)
2.4 MHz	3.6	177.4	169.4
1.2 MHz	2.5	106.6	100.4
600 kHz	2.1	53.7	49.4
300 kHz	2.0	38.5	32.6
150 kHz	1.9	24.0	23.7

SR: sparse reconstruction; DAS: delay-and-sum.

plate with two and three simulated damages. It should be noted that the A_0 mode is more sensitive to surface scatters 0 (such as glued rods) and S_0 mode is better in the detection of defects throughout the thickness (such as cut damage) (Su et al., 2006). In the present study, we chose S_0 mode for surface scatters detection to evaluate the methods for cut damage detection. Therefore, evaluation of methods is performed conservatively. Figures 17 and 18 show the results achieved from the experimental measurement.

Also, Figure 19 shows the results achieved by numerical simulations for the case of two 5-mm-long simulated crack on the plate.

It is clear from Figures 17 to 19 that the images reconstructed through the hybrid method are significantly improved in comparison with the DAS and SR methods when separately used. Also, as shown in Figure 18(b) in the SR method, the detection of a third damage location has almost totally failed, and some mistakes occur in the detection of damages in the both the SR and the DAS methods.
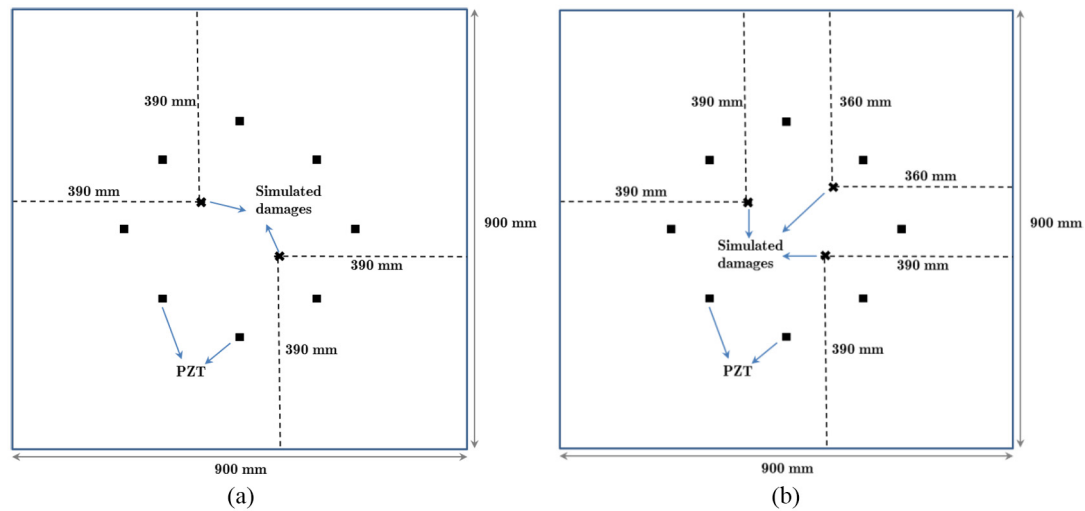
Figure 15. The configuration of the plates with (a) two damages and (b) three damages.

Figure 16. Experimental setup: (a) for two simulated damages and (b) for three simulated damages.
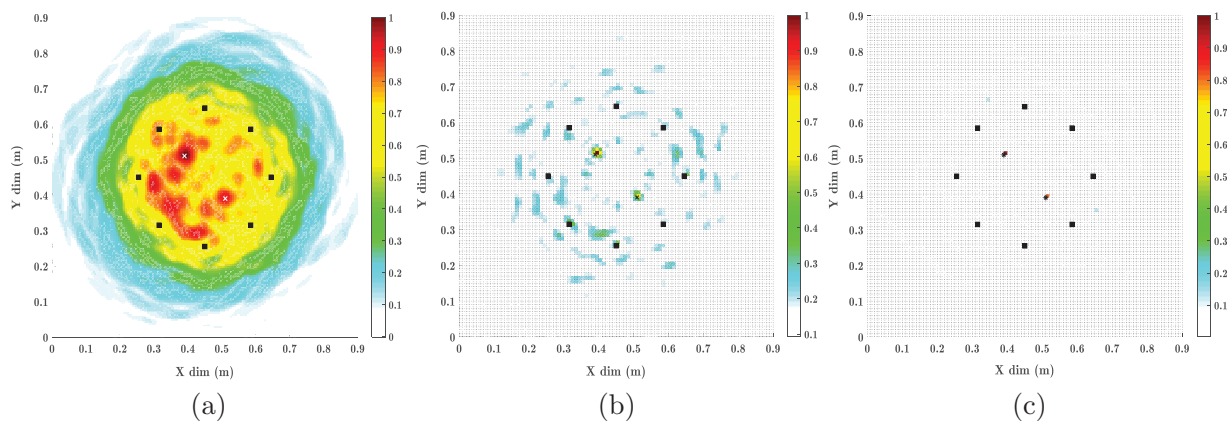

Figure 17. Images reconstructed through (a) DAS method, (b) SR method, and (c) hybrid method with the experimental signals for configuration (A). Damages are located at coordinates (39 cm, 51 cm) and (51 cm, 39 cm).

4. Conclusion

In this article for application in SHM, a hybrid method based on SR and DAS methods is proposed. The hybrid method increases the accuracy and robustness of the image reconstruction in the presence of multi-location damage and in cases with signal sampling frequency just below the Nyquist limit. To evaluate this method, experimental tests, as well as FEM numerical
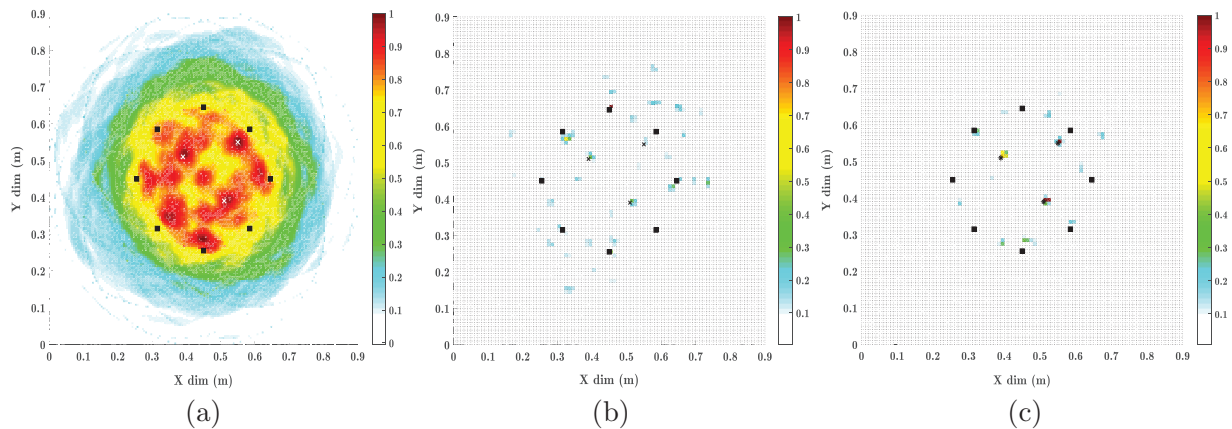
Figure 18. Images reconstructed through (a) DAS method, (b) SR method, and (c) hybrid method with the experimental signals for configuration (B). Damages are located at coordinates (39 cm, 51 cm), (51 cm, 39 cm), and (54 cm, 54 cm).
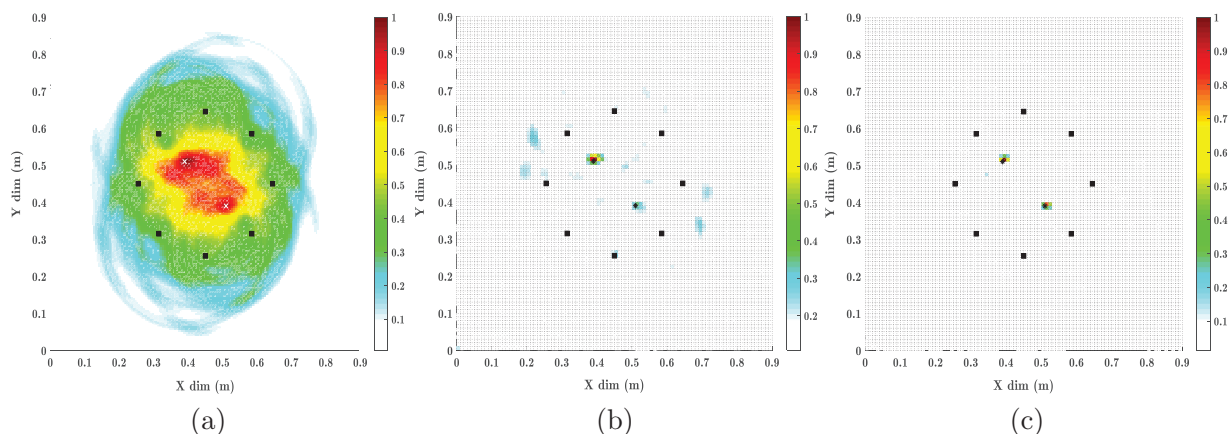

Figure 19. Images reconstructed through (a) DAS method, (b) SR method, and (c) hybrid method with the FEM simulation signals for the configuration (A) Damages are located at coordinates (39 cm, 51 cm) and (51 cm, 39 cm).

simulations, were performed on an aluminum plate. The results achieved from both experiments and numerical simulations show that using the hybrid method, one can obtain accurate and robust results with the reduced size dictionary matrix, which significantly decreases the cost and time of computation while also increasing the computational performance. Besides, in the hybrid method, the probability of multi-damage detection is much more than using either the SR or the DAS methods.

Declaration of conflicting interests

The authors declared no potential conflicts of interest with respect to the research, authorship, and/or publication of this article.

Funding

The author(s) received no financial support for the research, authorship, and/or publication of this article.

ORCID iD

Hossein M Navazi [iD] https://orcid.org/0000-0001-8508-3682

References

Alleyne DN and Cawley P (1992) The interaction of Lamb waves with defects. *IEEE Transactions on Ultrasonics, Ferroelectrics, and Frequency Control* 39(3): 381–397.

Balageas D, Fritzen CP and Güemes A (eds) (2006) *Structural Health Monitoring*, vol. 493. London: Iste.

Clarke T, Simonetti F and Cawley P (2010) Guided wave health monitoring of complex structures by sparse array systems: influence of temperature changes on performance. *Journal of Sound and Vibration* 329(12): 2306–2322.

Fan Z, Ni M, Zhu Q, et al. (2015) Weighted sparse representation for face recognition. *Neurocomputing* 151: 304–309.

Flinth A (2016) Optimal choice of weights for sparse recovery with prior information. *IEEE Transactions on Information Theory* 62(7): 4276–4284.

Flynn EB, Todd MD, Wilcox PD, et al. (2011) Maximum-likelihood estimation of damage location in guided-wave

structural health monitoring. *Proceedings of the Royal Society of London A: Mathematical, Physical and Engineering Sciences* 467(2133): 2575–2596.

Friedlander MP, Mansour H, Saab R, et al. (2012) Recovering compressively sampled signals using partial support information. *IEEE Transactions on Information Theory* 58(2): 1122–1134.

Giurgiutiu V (2005) Tuned Lamb wave excitation and detection with piezoelectric wafer active sensors for structural health monitoring. *Journal of Intelligent Material Systems and Structures* 16(4): 291–305.

Giurgiutiu V (2014) *Structural Health Monitoring with Piezoelectric Wafer Active Sensors*. Oxford: Academic Press.

Giurgiutiu V and Bao J (2004) Embedded-ultrasonics structural radar for in situ structural health monitoring of thin-wall structures. *Structural Health Monitoring* 3(2): 121–140.

Giurgiutiu V, Yu L, Bottai GS, et al. (2011) Structural health monitoring apparatus and methodology. US7881881B2 Patent.

Glisic B and Inaudi D (2008) *Fibre Optic Methods for Structural Health Monitoring*. Chichester: John Wiley & Sons.

Golato A, Santhanam S, Ahmad F, et al. (2016) Multimodal sparse reconstruction in guided wave imaging of defects in plates. *Journal of Electronic Imaging* 25(4): 043013.

Guo N and Cawley P (1993) The interaction of Lamb waves with delaminations in composite laminates. *The Journal of the Acoustical Society of America* 94(4): 2240–2246.

Hall JS and Michaels JE (2010) Minimum variance ultrasonic imaging applied to an in situ sparse guided wave array. *IEEE Transactions on Ultrasonics, Ferroelectrics, and Frequency Control* 57: 2311–2323.

Khajehnejad MA, Xu W, Avestimehr AS, et al. (2009) Weighted l1 minimization for sparse recovery with prior information. In: *2009 IEEE international symposium on information theory*, Seoul, South Korea, 28 June–3 July, pp. 483–487. New York: IEEE.

Khatir S, Wahab MA, Boutchicha D, et al. (2019) Structural health monitoring using modal strain energy damage indicator coupled with teaching-learning-based optimization algorithm and isogeometric analysis. *Journal of Sound and Vibration* 448: 230–246.

Lamb H (1917) On waves in an elastic plate. *Proceedings of the Royal Society of London A: Mathematical, Physical and Engineering Sciences* 93(648): 114–128.

Levine RM (2014) *Ultrasonic guided wave imaging via sparse reconstruction*. PhD Thesis, Georgia Institute of Technology, Atlanta, GA.

Levine RM and Michaels JE (2013) Model-based imaging of damage with Lamb waves via sparse reconstruction. *The Journal of the Acoustical Society of America* 133(3): 1525–1534.

Levine RM and Michaels JE (2014) Block-sparse reconstruction and imaging for lamb wave structural health monitoring. *IEEE Transactions on Ultrasonics, Ferroelectrics, and Frequency Control* 61(6): 1006–1015.

Michaels JE (2008) Detection, localization, and characterization of damage in plates with an in situ array of spatially distributed ultrasonic sensors. *Smart Materials and Structures* 17(3): 035035.

Michaels TE and Michaels JE (2004) Sparse ultrasonic transducer array for structural health monitoring. *AIP Conference Proceedings* 700(1): 1468–1475.

Mitra M and Gopalakrishnan S (2016) Guided wave based structural health monitoring: a review. *Smart Materials and Structures* 25(5): 053001.

Needell D, Saab R and Woolf T (2017) Weighted-minimization for sparse recovery under arbitrary prior information. *Information and Inference: A Journal of the IMA* 6(3): 284–309.

Purekar AS, Pines DJ, Sundararaman S, et al. (2004) Directional piezoelectric phased array filters for detecting damage in isotropic plates. *Smart Materials and Structures* 13(4): 838.

Quaegebeur N and Masson P (2012) Correlation-based imaging technique using ultrasonic transmit–receive array for non-destructive evaluation. *Ultrasonics* 52(8): 1056–1064.

Rose JL (2002) A baseline and vision of ultrasonic guided wave inspection potential. *Journal of Pressure Vessel Technology* 124(3): 273–282.

Samir K, Brahim B, Capozucca R, et al. (2018) Damage detection in CFRP composite beams based on vibration analysis using proper orthogonal decomposition method with radial basis functions and cuckoo search algorithm. *Composite Structures* 187: 344–353.

Sen D, Aghazadeh A, Mousavi A, et al. (2019) Sparsity-based approaches for damage detection in plates. *Mechanical Systems and Signal Processing* 117: 333–346.

Stepinski T, Uhl T and Staszewski W (eds) (2013) *Advanced Structural Damage Detection: From Theory to Engineering Applications*. Chichester: John Wiley & Sons.

Su Z, Ye L and Lu Y (2006) Guided Lamb waves for identification of damage in composite structures: a review. *Journal of Sound and Vibration* 295(3–5): 753–780.

Wang CH, Rose JT and Chang FK (2004) A synthetic time-reversal imaging method for structural health monitoring. *Smart Materials and Structures* 13(2): 415.

Wang W, Bao Y, Zhou W, et al. (2018) Sparse representation for Lamb-wave-based damage detection using a dictionary algorithm. *Ultrasonics* 87: 48–58.

Worlton DC (1956) *Ultrasonic testing with Lamb waves*. Report no. HW-45649 (Del.). Richland, WA: General Electric Co., Hanford Atomic Products Operation.

Wright W, Hutchins D, Jansen D, et al. (1997) Air-coupled Lamb wave tomography. *IEEE Transactions on Ultrasonics, Ferroelectrics, and Frequency Control* 44(1): 53–59.

Zhao X, Royer RL, Owens SE, et al. (2011) Ultrasonic Lamb wave tomography in structural health monitoring. *Smart Materials and Structures* 20(10): 105002.

Zhou YL, Maia NM, Sampaio RP, et al. (2017) Structural damage detection using transmissibility together with hierarchical clustering analysis and similarity measure. *Structural Health Monitoring* 16(6): 711–731.